Trends in Applied Spectroscopy
Vol. 9, 2012

Mini-Review

Steady-state photo-capacitance spectroscopy investigation of Carbon-related deep-level defects in AlGaN/GaN hetero-structures grown by MOCVD

Yoshitaka Nakano*

Institute of Science and Technology Research, Chubu University, 1200 Matsumoto, Kasugai, Aichi 487-8501, Japan

ABSTRACT

We have investigated C-related deep-level defects in AlGaN/GaN hetero-structures with different MOCVD growth conditions of GaN buffer layers, employing a steady-state photo-capacitance spectroscopy technique on their Schottky barrier diodes. The C impurity incorporation was enhanced with decreasing the growth temperature of the GaN buffer layer between 1120 and 1170°C. Acting in concert, three specific deep levels located at ~2.07, ~2.75, and ~3.23 eV below the conduction band were found to become dense significantly at the low growth temperature, presumably attributable to Ga vacancies and shallow C acceptors produced by the C incorporation into the GaN buffer layer. Additionally, from photo-assisted turn-on current recovery measurements, by using 390 and 370 nm long-pass filters, the recovery time became significantly faster due to inactivation of their corresponding deep-level traps. Therefore, the ~2.75 and ~3.23 eV levels related to the residual C impurity on N sites are strongly responsible for the carrier-trapping phenomena in the bulk region of the hetero-structures.

KEYWORDS: AlGaN/GaN hetero-structures, C impurity incorporation, deep-level defects, turn-on recovery characteristics

*nakano@isc.chubu.ac.jp

INTRODUCTION

AlGaN/GaN high electron mobility transistors (HEMTs), utilizing a two-dimensional electron gas (2DEG) produced at the hetero-interface, are the next generation of RF power transistor technology that offers the unique combination of higher power, higher efficiency and wider bandwidth than competing GaAs- and Si-based technologies [1]. However, the widespread implementation of GaN-based HEMTs is still restricted by reliability issues, particularly by the well-known current collapse phenomenon. The current collapse is the temporary reduction of the drain current following the application of high voltage and/or high power at both on- and off-state operations. That is, electrical charges trapped on the surface and/or in the bulk region of AlGaN/GaN hetero-structures modify the 2DEG concentration in the channel, which results in an increase in turn-on resistance and finally limits the switching characteristics of the devices [1]. Up to date, surface treatments on AlGaN top layer have already been reported to be effective in decreasing the current collapses by inactivating surface states of AlGaN [2]. Additionally, novel device structures with gate field plates have been demonstrated to decrease the current collapses by the modification of electric field at the gate edges [3]. However, at present, the current collapses have yet to be completely eliminated. Thus, in order to further develop the promising potential of GaN-based HEMTs, there is a need to perform basic

investigations of electronic deep-level defects in the bulk region of AlGaN/GaN hetero-structures from a viewpoint of device characteristics [4-8]. In our previous study, we had investigated a correlation between band-gap states and current collapses in two AlGaN/GaN hetero-structures with different current collapses, where the GaN and AlGaN layers were sequentially grown at the same temperatures of 1150 and 1100°C [9]. As a result, three specific deep-level defects located at ~2.07, ~2.75, and ~3.23 eV below the conduction band were found to be probably responsible for the current collapse phenomena of the AlGaN/GaN hetero-structures, and were likely associated with C impurity incorporation into AlGaN barrier and GaN buffer layers. In this study, focusing on the inevitable C impurity for metal-organic chemical vapor deposition (MOCVD) growth of AlGaN/GaN hetero-structures, we have screened C-related deep-level defects in the bulk region of the GaN buffer layer grown under different growth conditions and then investigated a more detailed relation between the C-related deep-level defects and turn-on recovery characteristics in the bulk region of AlGaN/GaN-based Schottky barrier diodes (SBDs) [10, 11].

EXPERIMENTAL

AlGaN/GaN hetero-structures used in this study were grown on *c*-plane sapphire substrates by MOCVD. Here, the growth temperature of the GaN buffer layer was varied at 1120, 1150, and 1170°C with keeping the AlGaN growth temperature of 1150°C, which are denoted by sample A, B, and C [10]. The growth pressure and V/III source ratio were kept constant. In addition, an AlGaN/GaN hetero-structure grown at 1150°C with low V/III ratio was also prepared, which is denoted by sample D. They consisted of an unintentionally doped 3 μm-thick GaN layer and an unintentionally doped 25 nm-thick AlGaN layer with an Al mole fraction of 24%. Their surface morphologies looked almost identical independent of the growth temperature, as determined from atomic force microscopic (AFM) observations (Figure 1). All the samples exhibited typical 2DEG properties, with a sheet carrier concentration of ~9×10^{12} cm^{-2} and a mobility of ~1200 cm^2/Vs, as determined by room-temperature (RT) Hall-effect measurements. The C concentrations of samples A, B, and C were uniformly ~6×10^{16}, ~2×10^{16}, and ~1×10^{16} cm^{-3} or less (the detection limit level), respectively, from secondary ion mass spectrometry (SIMS) measurements. Variable temperature photoluminescence (VT-PL) measurements were performed between 17 and 277 K to study optical properties of these samples. The PL was excited by the 313 nm bright line of a Hg-Xe lamp with an excitation power of ~1 W/cm^2. After growth, planar dot-and-plane (with ring-shaped-gap) SBDs were fabricated on these samples, using Ni as a Schottky metal. Ni metal dots were 1.0 mm in diameter. The gap between the ohmic and Schottky contacts was fixed at 20 μm. The fabricated Ni/AlGaN/GaN SBDs were characterized at RT by means of current-voltage (*I-V*), capacitance-voltage (*C-V*), and steady-state photo-capacitance spectroscopy (SSPC) measurements. The fabricated SBDs showed good rectifying characteristics from the *I-V* measurements in the dark. Photo and dark *C-V* measurements were performed at 100 kHz on the SBDs with and without white light illumination (λ >380 nm) from the back side with a 150 W Halogen lamp, using a long-pass filter. SSPC measurements were performed at 100 kHz, measuring photo-capacitance transients as a function of incident photon energy, from 0.78 eV (1600 nm) up to 4.0 eV (300 nm) [9-11]. The fabricated SBDs were illuminated from the back side with monochromatic light obtained from the same Halogen lamp coupled with a high resolution monochromator and higher-order cut filters. The photo-capacitance transients were recorded for 300 s after the onset of illumination. The SBDs were maintained under reverse biased conditions, where the measurement bias voltage, V_G, was suitably chosen to determine the discretionary probing depth range in the AlGaN/GaN hetero-structures. Prior to optical excitation, the deep levels were filled with electrons in the dark by applying a forward voltage pulse of +1.0 V with a pulse width of 1.0 s, followed by a 5.0 s delay, in order to reduce any possible thermal transient contributions to the photo-capacitance. In this study, the SSPC signal is defined as $\Delta C_{ss}/C_0$. Here, C_0 is the diode capacitance under the reverse biased condition in the dark, before the optical excitation, and ΔC_{ss} is

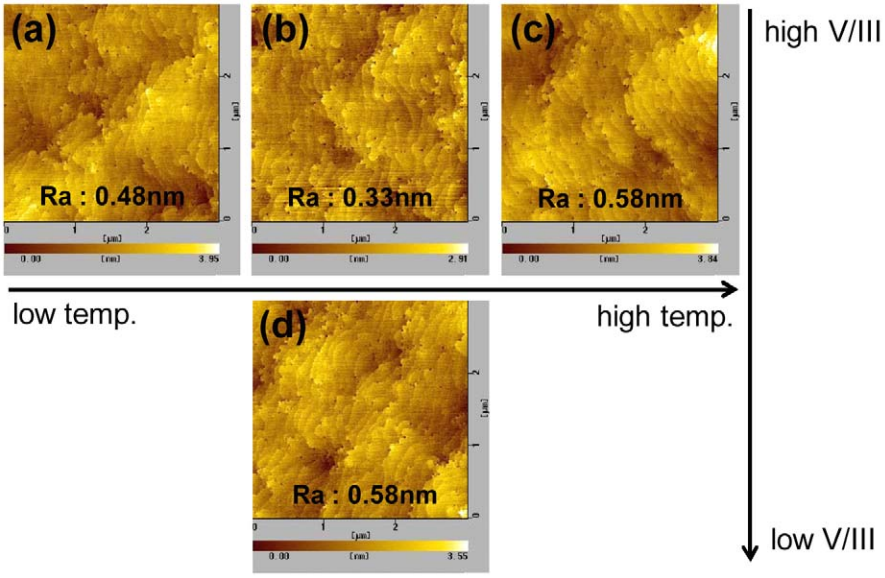

Figure 1. AFM images of (a) sample A, (b) sample B, (c) sample C, and (d) sample D.

the steady-state photo-capacitance, which is determined as a saturation value of their transients recorded at each wavelength. Additionally, for the simple estimation of carrier trapping in the bulk region, turn-on current recovery characteristics of sample B at V_G of +2.0 V after the off-state at V_G of -30 V were measured at RT under various optical illuminations using a 150 W Xe lamp coupled with three kinds of long-pass filters of 540, 390, and 370 nm [11]. Here, the stressing time under the off-state was fixed at 60 min. The reverse leakage current density under the off-state was ~90.9 mA/cm^2 in the dark.

RESULTS AND DISCUSSION

Figure 2 shows typical VT-PL spectra of samples A, B, and C. All the samples exhibit a broad yellow luminescence (YL) band around ~2.2 eV in addition to a band-edge (BE) emission of GaN around ~3.47 eV. This YL band is believed to be attributed to radiative transitions from a shallow donor to a deep acceptor, presumably a V_{Ga}-C_N complex involving a Ga vacancy and a C atom substituted for the N sites [12]. Additionally, samples B and C grown at the high growth temperatures show a strong shallow donor-acceptor pair (DAP) emission around ~3.28 eV, whereas sample A grown at the low growth temperature shows a C-related blue luminescence (BL) band centered at ~3.0 eV corresponding to radiative transitions from a C_{Ga} donor to a C_N acceptor, in addition to a relatively weak shallow DAP emission at ~3.28 eV [13]. Furthermore, the intensity ratios of YL to BE emissions at RT, YL/BE, are 3.30, 1.00, and 0.69 for samples A, B, and C, respectively. These experimental results support that the PL behavior significantly depends on the residual C content in the GaN buffer layer.

Typical dark and photo *C-V* characteristics of the Ni/AlGaN/GaN SBD samples are shown in Figure 3(a). A small increase in capacitance with illumination can be clearly observed in all the samples; compared to the dark *C-V* characteristics, the photo *C-V* ones shift a little more negatively in the partial pinch-off mode, reflecting an increase in 2DEG concentration due to deep-level photoemission near the AlGaN/GaN hetero-interface. Figure 3(b) shows the illumination-induced increase in capacitance, ΔC, as a function of V_G. Samples A, B, and C have maximum values at the V_G of -3.59, -3.82, and -3.77 V, respectively. From the integration of their corresponding ΔC peaks, the increased 2DEG concentrations on illumination, Δn_{2DEG}, are estimated to be at least 8.2x10^{10}, 7.6x10^{10}, and 7.2x10^{10} cm^{-2} for samples A, B, and C, respectively, and are considered to be optically excited from deep-level defects to the 2DEG at the AlGaN/GaN hetero-interfaces.

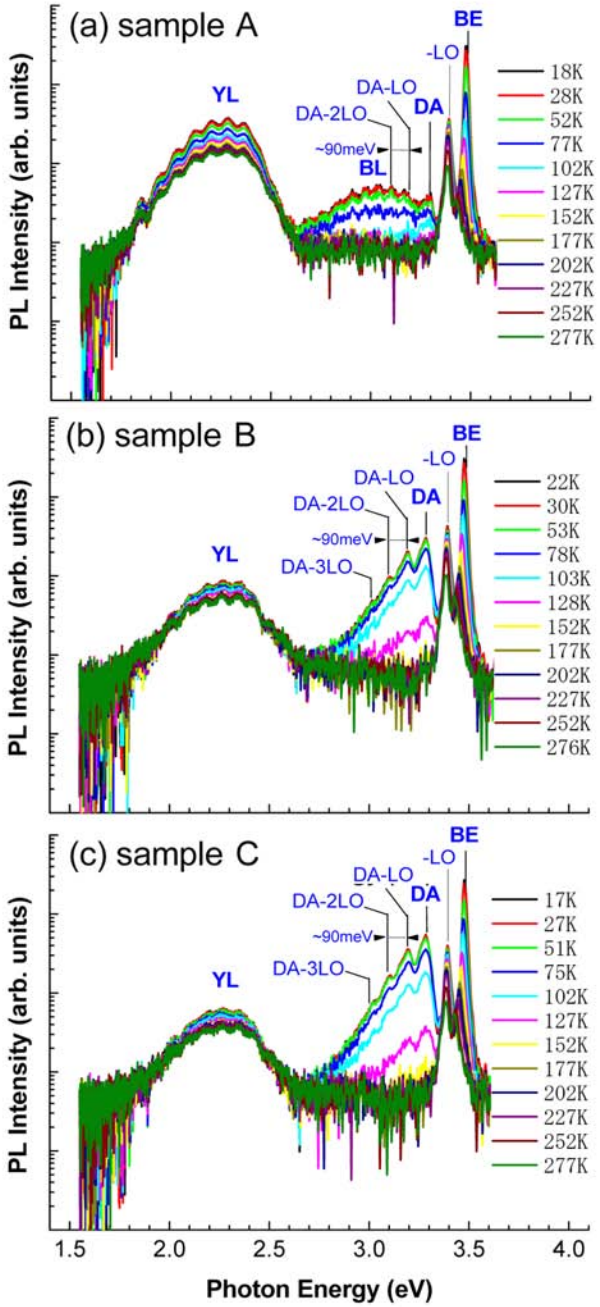

Figure 2. Variable temperature PL spectra of (a) sample A, (b) sample B, and (c) sample C.

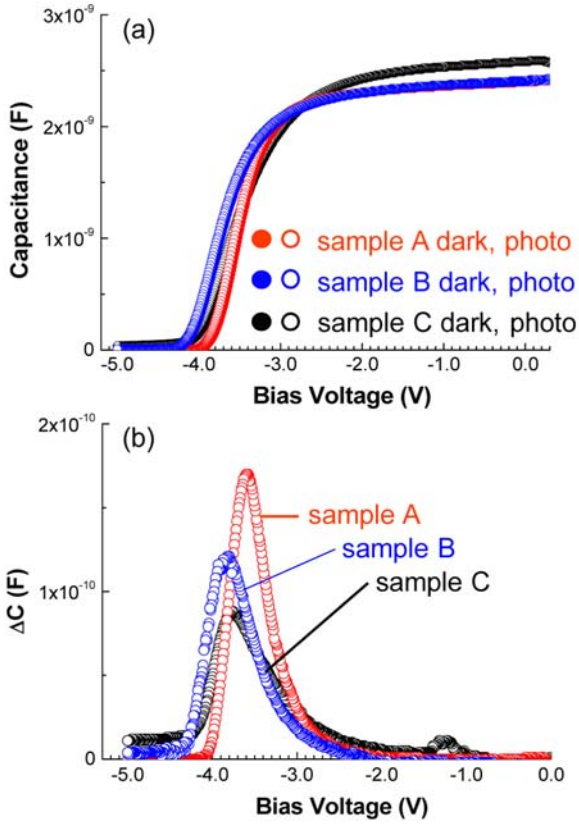

Figures 3. (a) Room-temperature dark and photo *C-V* characteristics of Ni/AlGaN/GaN SBDs based on samples A, B, and C. (b) Room-temperature Δ*C-V* characteristics of samples A, B, and C.

Assuming that all the samples are similar in deep-level concentration of the AlGaN layer due to the same growth condition, the difference of the increased 2DEG concentrations between samples A, B, and C is considered to come from the GaN buffer layer. The deep-level concentration in the GaN bulk region is probably increased with decreasing the growth temperature of the GaN buffer layer, i.e., the deep-level concentration significantly depends on the residual C content of the GaN buffer layer, as well as the YL/BE intensity ratio of the PL spectra.

Figure 4 shows typical room-temperature SSPC spectra of samples A, B, and C at their corresponding peak V_G of -3.59, -3.82, and -3.77 V, respectively, as determined from the *ΔC-V* characteristics in Figure 3(b). Here, by using the usual depletion approximation, all the probing depth ranges are in the GaN bulk region that are located around ~103, ~112, and ~82 nm from the top surface of the AlGaN layers for samples A, B, and C, respectively. All the samples show five photoemission states with their onsets at ~1.70, ~2.07, ~2.26, ~2.75, and ~3.23 eV (T1, T2, T3, T4, and T5) below the conduction band, in addition to the near-band-edge (NBE) emissions

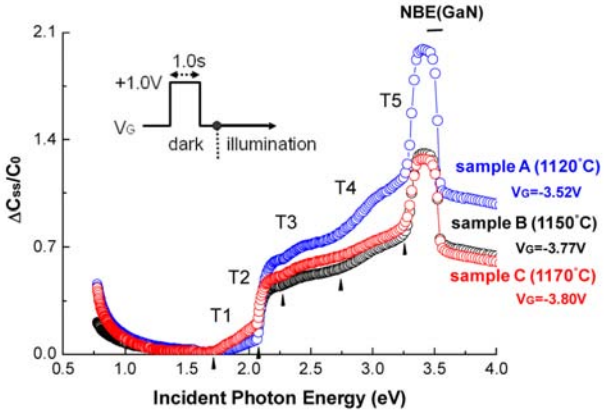

Figure 4. Room-temperature SSPC spectra of Ni/AlGaN/GaN SBDs based on samples A, B, and C.

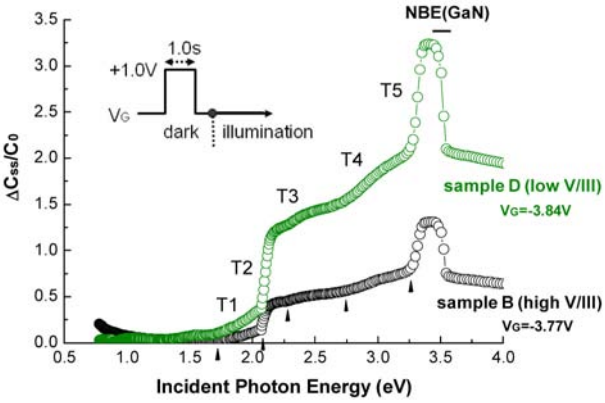

Figure 5. Room-temperature SSPC spectra of Ni/AlGaN/GaN SBDs based on samples B and D.

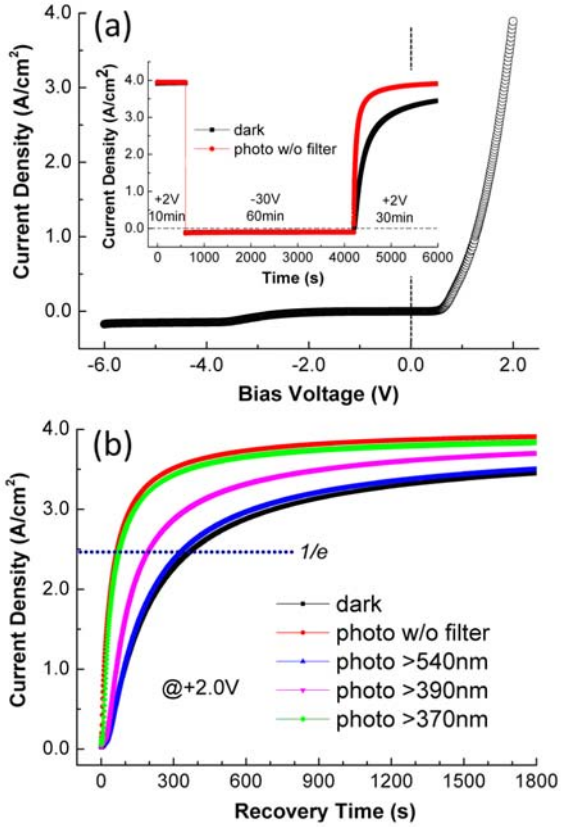

Figures 6. (a) *J-V* characteristics of Ni/AlGaN/GaN SBDs based on sample B. The inset shows current density behaviors under off-state and subsequent turn-on state at +2.0 V. (b) Turn-on current recovery characteristics after off-state under various optical illumination using long-pass filters of 540, 390, and 370 nm.

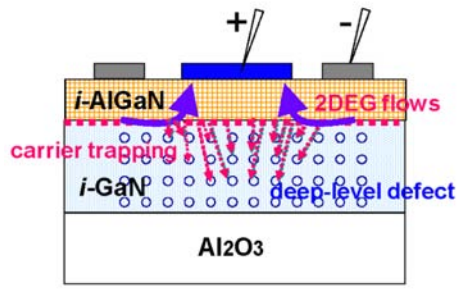

Figure 7. Trapping behavior of 2DEG carriers against forward electron flows under turn-on state.

from GaN at ~3.43 eV. These deep levels exhibit dominant process of electron emissions to the conduction band due to their positive photo-capacitance transients, and are almost identical to the deep-level defects that have been previously reported for AlGaN/GaN hetero-structures [8, 14, 15]. Additionally, negative photo-capacitance transients can be seen in the incident photon energy range between ~0.78 and ~1.35 eV for all the samples, which likely indicates the presence of a hole trap [16]. From the probing depth range, these deep levels turn out to stem from the GaN buffer layer. Among these deep levels, the ~2.07, ~2.75, and ~3.23 eV levels are seen to be significantly enhanced with decreasing the growth temperature of the GaN buffer layer, which is the same tendency as the *ΔC-V* and VT-PL results. Therefore, these specific levels are probably produced by the C impurity incorporation into the GaN buffer layer. In general, the C incorporation tends to be enhanced at the low growth temperature for MOCVD,

resulting in the deep-level formation of the residual C impurities and the Ga vacancies [16]. So, it is reasonable that sample A has higher deep-level concentrations than samples B and C, as revealed by the PL, ΔC-V, and SSPC measurements. The ~2.07, ~2.75, and ~3.23 eV levels observed in the SSPC spectra are considered to be related to the V_{Ga}- and the C-induced levels, that is, these deep-level defects are presumably attributable to V_{Ga} and/or V_{Ga}-O_N, V_{Ga}-C_N, and C_N, respectively [16-19]. Especially, the ~2.75 eV level is probably associated with the YL band observed in the PL spectra, as stated above.

We have also investigated the electronic band-gap states in AlGaN/GaN hetero-structures with different V/III source ratios of the GaN buffer growth in view of the C impurity incorporation. As shown in Figure 5, with decreasing the V/III ratio, the C incorporation is found to become significant, which results in enhanced formation of the ~2.07, ~2.75, and ~3.23 eV levels. This is in good agreements with the experimental results as stated above. The generation behavior of these specific deep-levels seems in conjunction with each other due to their common origin of the C impurity incorporation [9, 10]. Thus, it is difficult to distinguish these deep-levels from a viewpoint of the carrier trapping in AlGaN/GaN hetero-structures. In this study, in order to separate the effect of each deep-level defect on the carrier trapping in the bulk region, turn-on current recovery characteristics of sample B after the off-state were evaluated under various optical illuminations, as shown in the inset of Figure 6(a) [11]. On the Ni/AlGaN/GaN-based SBDs fabricated, the turn-on current recovery characteristics are dominantly determined by the thermionic emission from the Schottky barrier, as seen in the current density-voltage (J-V) characteristics of Figure 6(a). Assuming that numerous deep-level traps are present in the bulk region under the Schottky junction, they continue to capture 2DEG carriers against the forward current flows toward their thermally steady-state levels under the turn-on state after the off-state (Figure 7), resulting in increasing the turn-on recovery time. That is, at first, the deep-level traps should release trapped electrons during the off-state and then start to capture 2DEG carriers under the turn-on state. Thus, the turn-on recovery time strongly depends on how many 2DEG carriers can be captured at the deep-level traps in the bulk region against the current flows. In this study, we used three kinds of long-pass filters with their cut-off wavelengths of 540, 390, and 370 nm, corresponding to photon energies of 2.30, 3.18, and 3.35 eV. The turn-on recovery time is defined as an exponential time constant for the current recovery characteristics. As shown in Figure 6(b), the recovery time in the dark is ~372 s, and the slow value is probably due to the 2DEG carrier-trapping at the deep-level traps in the bulk region under the turn-on state. In sharp contrast, the recovery time significantly shortens down to ~67 s by the optical illumination without any filters. This phenomenon implies that all the deep-level traps become inactive against the carrier trapping due to absorbing the white-light photon energies. Additionally, the recovery time is found to be mostly unchanged by the optical illumination with the 540 nm filter, compared to that in the dark, which suggests that the ~2.07 eV level is not related to the turn-on recovery characteristics. On the other hand, the recovery time tends to become significantly shorter under the illuminations with the 390 and 370 nm filters. These experimental results indicate that the ~2.75 and ~3.23 eV levels are strongly responsible for the turn-on recovery characteristics, that is, they behave as deep-level traps in the bulk region. Considering that these deep-level traps are closely related to the substitutional C_N on N sites, the residual C impurity on the N sites would play an important role in the carrier-trapping phenomena in the bulk region of AlGaN/GaN hetero-structures [14].

CONCLUSION

The planar Ni/AlGaN/GaN-based SBDs with different MOCVD growth conditions have been characterized by C-V, SSPC, and photo-assisted turn-on current recovery measurements in view of C impurity incorporation into GaN buffer layers. Three specific deep-level defects were found to be located at ~2.07, ~2.75, and ~3.23 eV below the conduction band, which are presumably attributable to V_{Ga} and/or V_{Ga}-O_N, V_{Ga}-C_N, and C_N in the GaN buffer layer. Among them, the ~2.75 and ~3.23 eV levels turn out to be strongly

responsible for the carrier-trapping phenomena in the bulk region of AlGaN/GaN hetero-structures.

ACKNOWLEDGEMENTS

A part of this work was supported by the Grant-in-Aid for Scientific Research (C) and the "Tokai Region Nanotechnology Manufacturing Cluster" in the Knowledge Cluster Initiative (the Second Stage) of the Ministry of Education, Culture, Sports, Science and Technology (MEXT), Japan.

REFERENCES

1. Bradley, S. T., Young, A. P., Brillson, L. J., Murthy, M. J., Schaff, W. J. and Eastman, L. F. 2001, IEEE Trans. Electron Devices, 48, 412.
2. Luo, B., Johnson, J. W., Kim, J., Mehandru, R. M., Ren, F., Gila, B. P., Onstine, A. H., Abernathy, C. R., Pearton, S. J., Baca, A. G., Briggs, R. D., Shul, R. J., Monier, C. and Han, J. 2002, Appl. Phys. Lett., 80, 1661.
3. Ando, Y., Okamoto, Y., Miyamoto, H., Nakayama, T., Inoue, T. and Kuzuhara, M. 2003, IEEE Electron Device Lett., 24, 289.
4. Arulkumaran, S., Egawa, T., Ishikawa, H. and Jimbo, T. 2002, Appl. Phys. Lett., 81, 3073.
5. Klein, P. B. 2002, J. Appl. Phys., 92, 5498.
6. Zhang, A. P., Rowland, L. B., Kaminsky, E. B., Tilak, V., Grande, J. C., Teetsov, J., Vertiatchikh, A. and Eastman, L. F. 2003, J. Electron. Mater., 32, 388.
7. Fang, Z.-Q., Look, D. C., Kim, D. H. and Adesida, I. 2005, Appl. Phys. Lett., 87, 182115.
8. Nakano, Y., Irokawa, Y. and Takeguchi, M. 2008, Appl. Phys. Express, 1, 091101.
9. Nakano, Y., Irokawa, Y., Sumida, Y., Yagi, S. and Kawai, H. 2010, Phys. Stat. Sol. RRL, 4, 374.
10. Nakano, Y., Irokawa, Y., Sumida, Y., Yagi, S. and Kawai, H. 2011, Electrochem. Solid-State Lett., 15, HH44.
11. Nakano, Y., Irokawa, Y., Sumida, Y., Yagi, S. and Kawai, S. 2012, J. Appl. Phys., 112, 106103.
12. Niebuhr, R., Bachem, K., Bombrowski, K., Maier, M., Plerschen, W. and Kaufmann, U. 1995, J. Electron. Mater. 24, 1531.
13. Lee, S. M., Belkhir, M. A., Zhu, X. Y., Lee, Y. H., Hwang, Y. G. and Frauenheim, T. 2000, Phys. Rev. B, 61, 16033.
14. Klein, P. B., Binari, S. C., Ikossi, K., Wickenden, A. E., Koleske, D. D. and Henry, R. L. 2001, Appl. Phys. Lett., 79, 3527.
15. Armstrong, A., Chakraborty, A., Speck, J. S., DenBaars, S. P., Mishra, U. K. and Ringel, S. A. 2006, Appl. Phys. Lett., 89, 262116.
16. Fang, Z.-Q., Claflin, B., Look, D. C., Green, D. S. and Vetury, R. 2010, J. Appl. Phys., 108, 063706.
17. Armstrong, A., Arehart, A. R., Moran, B., DenBaars, S. P., Mishra, U. K., Speck, J. S. and Ringel, S. A. 2004, Appl. Phys. Lett., 84, 374.
18. Armstrong, A., Arehart, A. R., Green, D., Mishra, U. K., Speck, J. S. and Ringel, S. A. 2005, J. Appl. Phys., 98, 053704.
19. Son, N. T., Hemmingsson, C. G., Paskova, T., Evans, K. R., Usui, A., Morishita, N., Ohshima, T., Isoya, J., Monemar, B. and Janzén, E. 2009, Phys. Rev. B, 80, 153202.